ELSEVIER

Ceramics International 33 (2007) 373–378

CERAMICS INTERNATIONAL

www.elsevier.com/locate/ceramint

Isothermal and cycle properties of EB-PVD yttria-partially-stabilized zirconia thermal barrier coatings at 1150 and 1300 °C

Shuqi Guo [a,*], Yutaka Kagawa [a,b]

[a] National Institute for Materials Science, 1-2-1 Sengen, Tsukuba, Ibaraki 305-0047, Japan
[b] Research Center for Advanced Science and Technology, The University of Tokyo, 4-6-1 Komaba, Meguro-ku, Tokyo 153-8505, Japan

Received 1 August 2005; received in revised form 9 September 2005; accepted 4 October 2005
Available online 18 January 2006

Abstract

Phase evolution in an electron beam physical vapor deposited (EB-PVD) yttria-partially-stabilized zirconia thermal barrier coating (TBC) was examined during isothermal and cycle ageing at 1150 and 1300 °C in ambient air. The nonequilibrium tetragonal phase was transformed to tetragonal, and/or cubic and/or monoclinic phase during isothermal and cycle ageing, and these changes of phase depended on ageing temperature, duration and history as well as residual stress in TBC.

Keywords: D. Y_2O_3; D. ZrO_2; Phase transformation; Residual stress; Isothermal and cycle ageing

1. Introduction

Thermal barrier coatings (TBCs) have been used for almost three decades to extend the life of combustors, augmentors and, more recently, stationary turbine components [1,2]. Among them, air plasma-sprayed (APS) and electron beam physical vapor deposited (EB-PVD) yttria-partially-stabilized zirconia TBCs have been widely studied in recent years because of their potential possibilities to substantially extend turbine lives and improve engine efficiencies [2–7]. In particular EB-PVD TBCs recently have received attention because the coatings are expected to overcome APS TBCs in mechanical performance [5–7]. This superior mechanical performance is attributable to a specific columnar structure of the EB-PVD TBCs. This columnar structure allows superior tolerance against straining and thermoshock, as a result of the individual columns of the columnar structure preventing the build-up of tensile stresses and match of the thermal expansion coefficient differences between the TBC layer and the substrate.

On the other hand, the phase stability in the EB-PVD TBCs during service is another key factor in controlling the TBCs life. It is well-known that zirconia shows three possible crystallographic phases [8]: (i) low temperature monoclinic phase; (ii) intermediate temperature tetragonal phase; and (iii) high temperature cubic phase. The tetragonal to monoclinic phase transformation is diffusionless and the transformation results in a significant volume expansion. Although the high temperature cubic phase in zirconia can be fully stabilized by addition of Y_2O_3, these compositions are seldom used for TBCs because they exhibit a poor cyclic life. Recently, Y_2O_3 partially stabilized ZrO_2 (6–8 wt.% Y_2O_3) is the most commonly and typically used material for APS and EB-PVD TBCs [1–7]. However, these materials show insufficient phase stability at temperatures [7,9–12]: the as-deposited nonequilibrium tetragonal (t′) phase in the Y_2O_3 partially-stabilized ZrO_2 TBCs was decomposed during ageing. The t′ phase would transformed to a mixture of the tetragonal (t) + cubic (c) + monoclinic (m) phases as well as a mixture of the tetragonal (t) + cubic (c) phases. This is closely linked with location, ageing temperature, heating rate, cooling rate, exposure history, deposition process and residual stress in TBC. Among these possible phase transformations, the t → m phase transformation results in a significant volume change, and subsequently, high stresses within the TBC. This phase transformation contributed to rapid spallation of the TBC from the substrate during temperature variation [13]. Therefore, it is required for the EB-PVD TBCs to learn whether the t → m phase transformation occurred on cooling from service temperature as

* Corresponding author. Tel.: +81 29 859 2223; fax: +81 29 859 2401.
E-mail address: GUO.Shuqi@nims.go.jp (S. Guo).

0272-8842/$32.00
doi:10.1016/j.ceramint.2005.10.005

well as to examine the phase evolution behavior. Although the phase transformation in the EB-PVD TBCs during isothermal and cycle ageing is being studied, these studies are not enough to know well phase transformation behavior in the EB-PVD-TBC system. In particular the effect of residual stress on the phase transformation is little known. The present study presents the X-ray diffraction results of the phase transformation in an EB-PVD Y_2O_3 partially-stabilized ZrO_2 TBC during the isothermal and cycle ageing at 1150 and 1300 °C. Also, the correlation of residual stress in TBC to the phase transformation is discussed.

2. Experimental procedure

The material used in this study was prepared by an electron beam physical vapor depositing 7.1 wt.% Y_2O_3 stabilized ZrO_2 powder on a MA738LC nickel-based superalloy substrate with a NiCOCrAlY bond coat overlayer. The bond coat was deposited by a low-pressure plasma spray deposition to a thickness of ∼100 μm, and has an overall composition of 32 wt.% Ni, 21 wt.% Cr, 8 wt.% Al, 0.5 wt.% Y, with the balance Co. The bond coat surface deposited was then polished up to #1200 before the TBC deposition. The preheating temperature of the substrate was 1268 K. Typically, the EB-PVD-processed TBC layer was approximately 200 μm thick. This EB-PVD TBC system was supplied by the JFCC (Japan Fine Ceramics Center, Nagoya, Japan). The microstructure of the as-deposited EB-PVD TBC system is shown in Fig. 1. The TBC system consists of the following four layers: (i) superalloy substrate; (ii) bond coat layer; (iii) thin thermally grown oxide (TGO) layer; and (iv) Y_2O_3-stabilized ZrO_2 TBC layer. The EB-PVD TBC layer shows a typical columnar structure. The TGO layer is ∼0.5 μm thick and is present between the TBC layer and the bond coat layer.

To examine phase transformation behavior of the TBC layer, the obtained EB-PVD TBC specimens were exposed to isothermal and cycle ageing in air. The isothermal ageing test was carried out at 1150 and 1300 °C for 10, 50 and 100 h. During this procedure, the heating rate and cooling rate were set to be 8 and 6 °C/min, respectively. The cycle ageing test consisted of a 60 min exposure at 1150 °C and a 10 min hold time at 25 °C with heating and cooling rates of 115 °C/min. This procedure was repeated 10, 50 and 100 times, in order to compare with the isothermal ageing. Phase compositions in the as-deposited, isothermally and cyclically exposed EB-PVD TBC layer were examined by using an X-ray diffractometry (XRD; 40 kV, 100 mA, Cu Kα radiation).

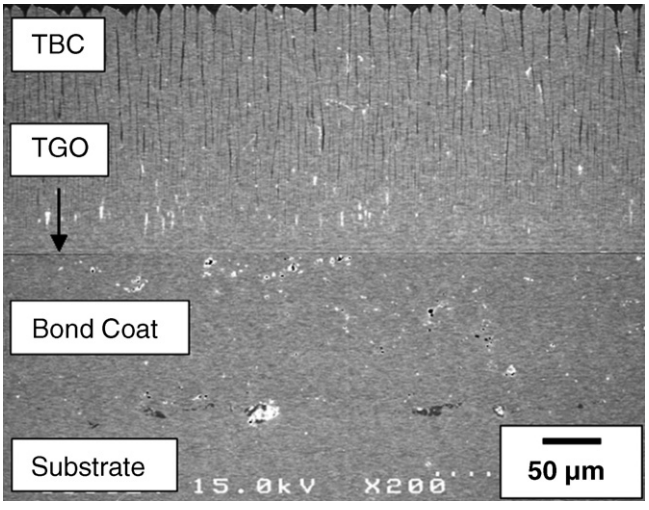

Fig. 1. A typical SEM micrograph of the cross-section for the as-deposited EB-PVD TBC system, showing (i) superalloy substrate; (ii) bond coat; (iii) TGO layer; and (iv) TBC layer with typical columnar structure.

3. Results and discussion

Fig. 2 shows X-ray diffraction patterns of the top surface for the as-deposited EB-PVD TBC specimen. In the low-angle diffraction region of $2\theta = 28–38°$ (Fig. 2(a)), only (0 0 2) and (2 0 0) peaks of the tetragonal phase were detected, while (1 1 1) peaks of this phase did not appear. Additionally, the peaks of cubic and/or monoclinic phase were not detected. On the other hand, in the high-angle diffraction region of $2\theta = 71–77°$ (Fig. 2(b)), only (0 0 4) and (4 0 0) peaks of the tetragonal phase were detected. Detection of (0 0 2) peaks of the tetragonal phase instead of (1 1 1) peaks in the low-angle diffraction region has reported previously for the as-deposited TBC layer. Wada et al. [14] showed that the formation of crystallographic textures in the EB-PVD TBC remarkably depended on the preheating temperature of the substrate. They find that the peaks of (1 1 1) appear in $2\theta = 28–38°$ as the preheating temperature of the substrate was 925 K, whereas the peaks of (2 0 0) and (4 0 0) appear in $2\theta = 28–38°$ and $2\theta = 71–77°$, respectively, as the preheating temperature was above 1211 K. A similar cause is

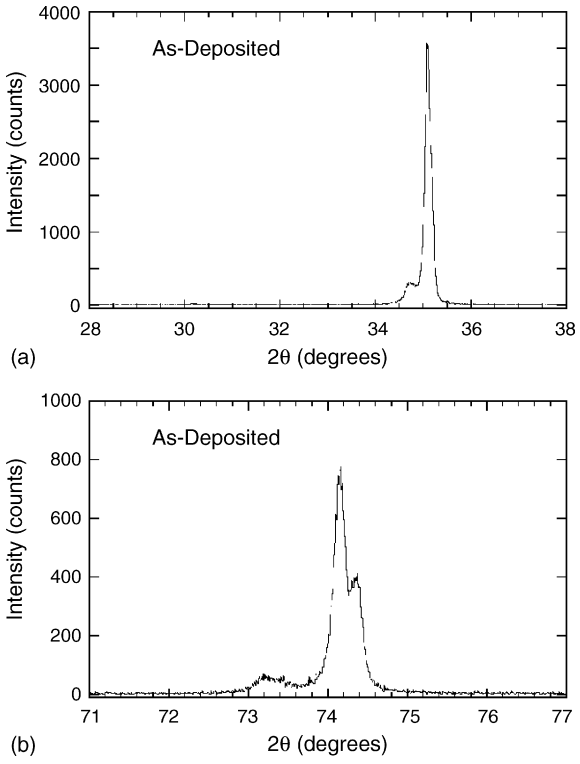

Fig. 2. X-ray diffraction patterns of the top surface for the as-deposited EB-PVD TBC system.

expected for the TBC layer in the EB-PVD TBC system investigated in the present study because the preheating temperature (1268 K) of the substrate exceeded 1211 K.

The lattice parameters of the tetragonal phase were determined from the XRD patterns in the region of $2\theta = 71–77^\circ$, and they were found to be $a = 5.1104$ Å and $c = 5.1652$ Å with the c/a ratio of 1.0107. The amount of Y_2O_3 in the tetragonal phase is given by [15]

$$\text{wt.\%YO}_{1.5} = \frac{1.0185 - c/a}{0.001107} \quad (1)$$

The Y_2O_3 content in the tetragonal phase was determined to be approximately 7.1 wt.%. The obtained Y_2O_3 content in the tetragonal phase was higher than 6 wt.% Y_2O_3 that was critical for obtaining the metastable "nontransformable" tetragonal (t′) phase. Thus, the tetragonal phase detected in the present study was identified to be the nonequilibrum tetragonal (t′) phase and this phase is the metastable nontransformable.

Fig. 3 shows X-ray diffraction patterns of the top surface for the EB-PVD TBC after the isothermal ageing at 1150 and 1300 °C for 10, 50 and 100 h. For the EB-PVD TBC exposed at 1150 °C, only (0 0 2) and (2 0 0) peaks were detected in the low-angle diffraction region of $2\theta = 28–38^\circ$ (Fig. 3(a)). This is quite similar to that of the as-deposited EB-PVD TBC, however, the intensity of the peaks was lower than that of the as-deposited TBC (Fig. 2(a)). This suggests that the phase transformation in the TBC layer occurred during isothermal ageing. In the high-angle diffraction region of $2\theta = 71–77^\circ$

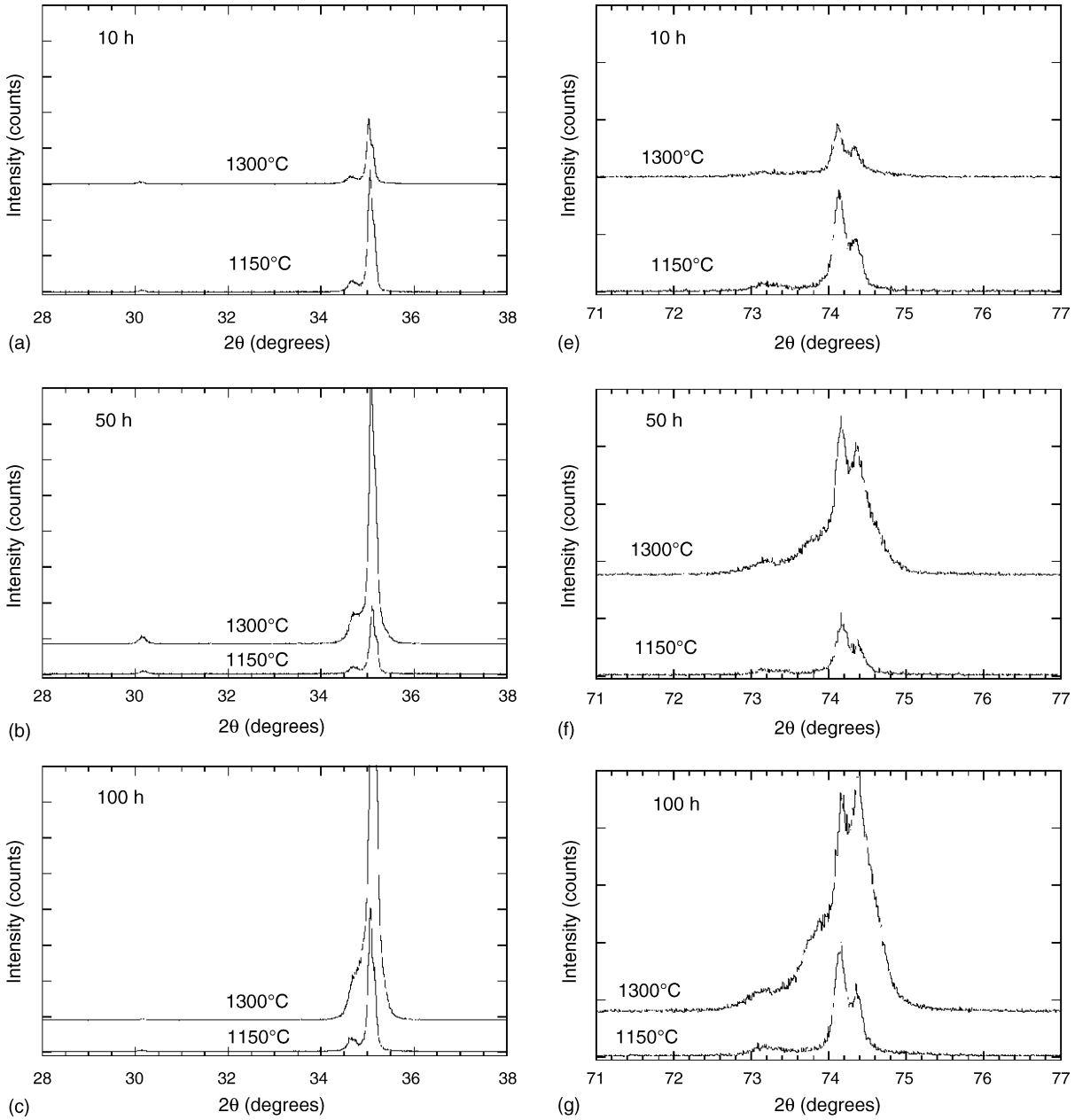

Fig. 3. X-ray diffraction patterns of the top surface for the EB-PVD TBC system after isothermal ageing at 1150 and 1300 °C for (a) and (e) 10 h; (b) and (f) 50 h; (c) and (g) 100 h.

(Fig. 3(e)), on the other hand, low-stabilizer tetragonal phase (t1) and the higher stabilizer-containing tetragonal (t2) phase were clearly detected, but no cubic phase was detected. For t2 phase the lattice parameters, a and c, were determined using the t2 peaks: $a = 5.1128$ Å and $c = 5.1676$ Å with $c/a = 1.0107$. The corresponding Y_2O_3 content in the phase was determined to be approximately 7.0 wt.%. For t1 phase the lattice parameters, a and c, were determined to be $a = 5.0952$ Å and $c = 5.1744$ Å with $c/a = 1.0155$. The corresponding Y_2O_3 content in the phase was 2.7 wt.% and this value was slightly higher than the Y_2O_3 solubility (≈2.3 wt.%) for equilibrium phase diagram [8,11]. This suggests that nonequilibrum tetragonal (t′) phase decomposed to t1 and t2 phases after isothermal ageing of 10 h at 1150 °C. After isothermal ageing of 50 h, however, (1 1 1) peak of the cubic phase was also detected in (1 1 1) region accompanying with t1 and t2 phase (Fig. 3(b)), but no peak of (4 0 0) was detected in (4 0 0) region of c phase (Fig. 3(f)). After isothermal ageing of 100 h, similar phase composition was detected (Fig. 3(c) and (g)). The Y_2O_3 content in the c phase could be calculated using the following equation, based on value of the Aleksandrov model [12]

$$\text{mol.\%}Y_2O_3 = 770.59a^2 - 7631.6a + 18877 \quad (2)$$

where a is the lattice constant of the cubic phase. The lattice parameter, a, of c phase was determined to be $a = 5.1270$ Å and 5.1302 Å for the isothermally aged TBC for 50 and 100 h, respectively. The corresponding Y_2O_3 content in c phase was 9.1 and 11.3 wt.%. This indicated that the c phase is a nonequilibrum phase containing low Y_2O_3 content because the Y_2O_3 content in the equilibrum c phase at 1150 °C is approximately 18 wt.% [8,11]. Conversely, the Y_2O_3 content in t2 phase initially decreased with ageing time, but almost changed in the range of 50 and 100 h: 5.8 and 5.9 wt.% after ageing of 50 h and 100 h, respectively. The Y_2O_3 content in t1 phase remained nearly constant with ageing time in the range studied (10–100 h), however. This means that the nonequilibrum phase t′ partially transformed to c phase during further isothermal ageing. In the contrast, after isothermal ageing at 1300 °C, t1, t2 and c phases were detected in any instance. The Y_2O_3 content in t2 phase decreased with ageing time, as shown in Fig. 4. After

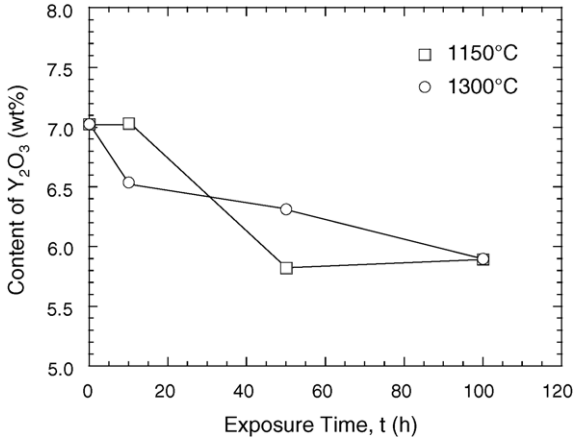

Fig. 4. Y_2O_3 content in the t-phase after isothermal ageing, as a function of temperature and time.

isothermal ageing of 10 h, the Y_2O_3 content in c phase was 14.8 wt.%, whereas after ageing of 50 and 100 h the Y_2O_3 content was about 12.6 and 12.5 wt.%, respectively. These values approached the Y_2O_3 solubility for the equilibrum c phase at 1300 °C [8]. In addition, in the high-angle diffraction region of $2\theta = 71$–$77°$, the relative intensity of (4 0 0) peak of c phase increased with time. This means that the c phase amount increased with ageing time. Thus, the nonequilibrum t′ phase in the as-deposited TBC decomposed to the t1 phase, t2 phase and c phase during isothermal ageing at 1300 °C. However, monocline phase was not detected in any instance after isothermal ageing at 1150 and 1300 °C up to 100 h.

Fig. 5 shows X-ray diffraction pattern of the top surface for the cycle aged EB-PVD TBC at 1150 °C for 10, 50 and 100 cycles. Differing from isothermal ageing, no cubic phase was detected in any instance. After cycle ageing of 10 and 50 cycles, the equilibrum t1 phase and the t2 phase were detected, resulting from decomposition of the nonequilibrum t′ phase in the as-deposited EB-PVD TBC. The lattice parameters of the tetragonal phase (t2) were determined to be $a = 5.1120$ Å and $c = 5.1676$ Å with $c/a = 1.0111$ for cycle ageing of 10 cycles, and $a = 5.1080$ Å and $c = 5.1680$ Å with $c/a = 1.0117$ for cycle ageing of 50 cycles. The corresponding Y_2O_3 content in t2 phase was 6.7 and 6.1 wt.%, respectively. After cycle ageing of 100 cycles, however, no t1 phase peak was detected, but significant monocline phase peak (0 2 0) and t2 phase were detected. The lattice parameters of the t2 were determined to be $a = 5.1132$ Å and $c = 5.1700$ Å with $c/a = 1.0111$. The corresponding Y_2O_3 content in t2 phase was 6.7 wt.%. The change of the Y_2O_3 content in t2 phase with number of cycles is shown in Fig. 6. The detection of the m phase suggests that the t1 phase transforms to m phase on cooling. The phase transformation of tetragonal to monocline in TBC material after cycle ageing has examined by some investigators [12,13]. They concluded that the tetragonal to monocline transformation is affected not only by Y_2O_3 composition, but also by the grain size of the tetragonal phase and by stress state within the material.

In the TBC layer studied, it has been reported that the residual stress was present and related to ageing history [16]. This suggests that the residual stress may affect the phase transformation after isothermal and cycle ageing. The biaxial stress in the TBC layer can be measured by the Raman shift for the TBC coatings at various states [16,17]. In the present study, similar measurement was conducted at room temperature in ambient air for the EB-PVD TBC layer after isothermal and cycle ageing. The measurement was done using a specially designed micro-Raman spectrophotometer (NRS-1000, Special version, JASCO Co., Tokyo, Japan); details of the measurement were reported elsewhere [17]. The data obtained on the top surface reveal that the residual stress in the studied TBC layer is compressive and the stress is larger for cycle ageing than for isothermal ageing under the same duration at high temperature, as shown in Fig. 7. Note that the residual stress in the TBC layer is dependent on location [16,17]: the stress is more compressive near the TGO/TBC interface and decreases towards the surface. Here the average values of the residual stress in TBC layer were measured. Furthermore, the residual stress in the TBC

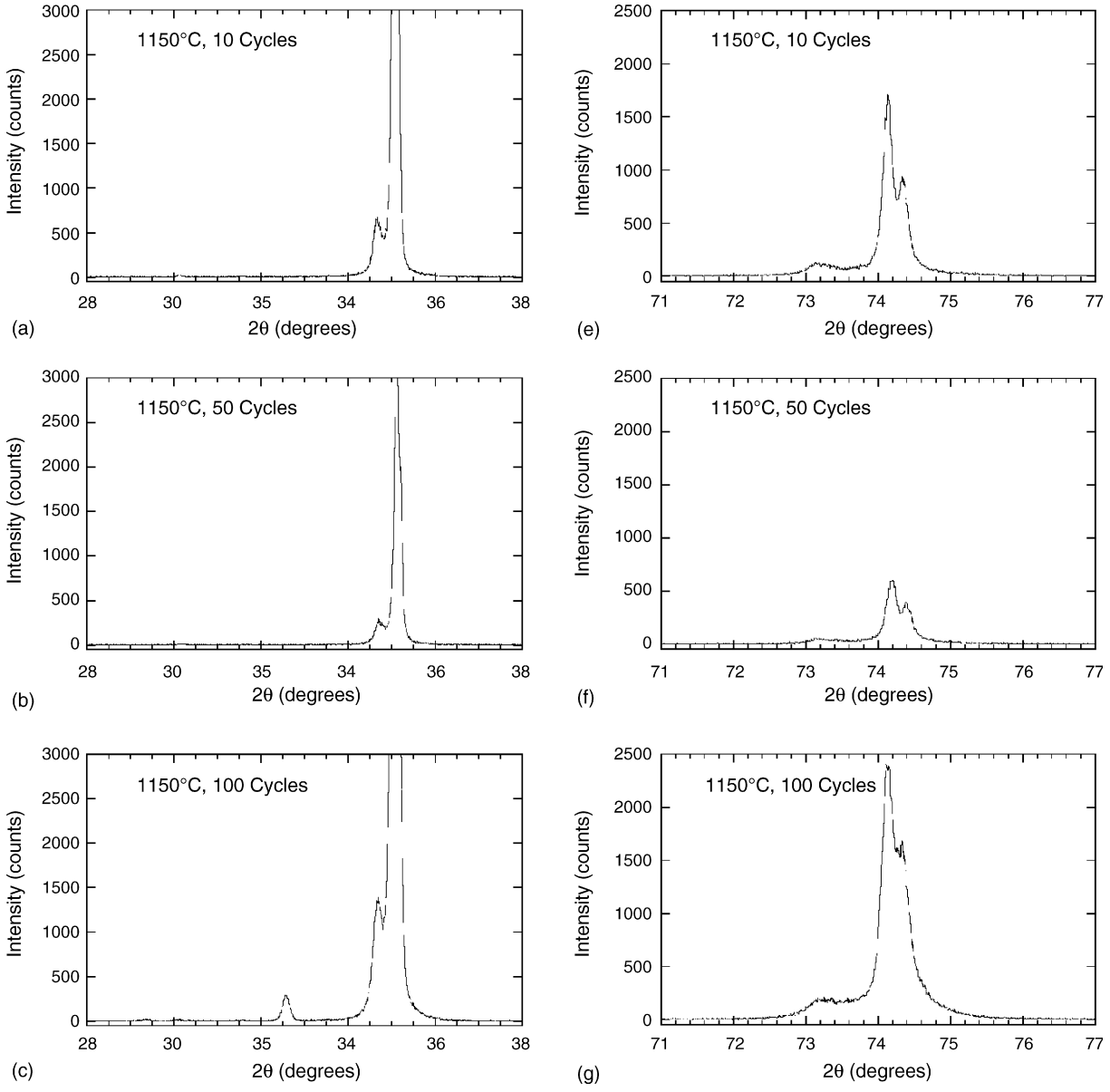

Fig. 5. X-ray diffraction patterns of the top surface for the EB-PVD TBC system after cycle ageing at 1150 °C for (a) and (e) 10 cycles; (b) and (f) 50 cycles; (c) and (g) 100 cycles.

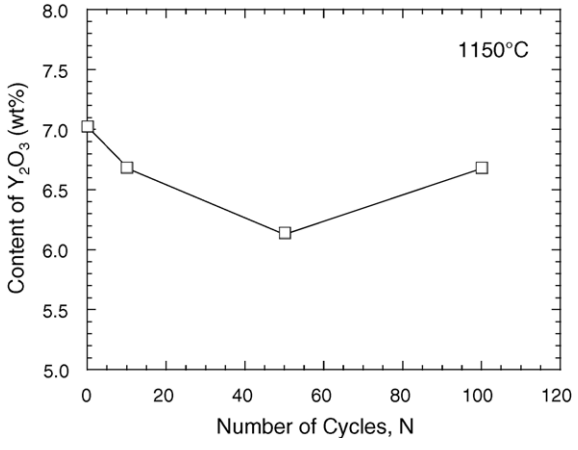

Fig. 6. Y_2O_3 content in the t-phase after cycle ageing, as a function of number of cycles.

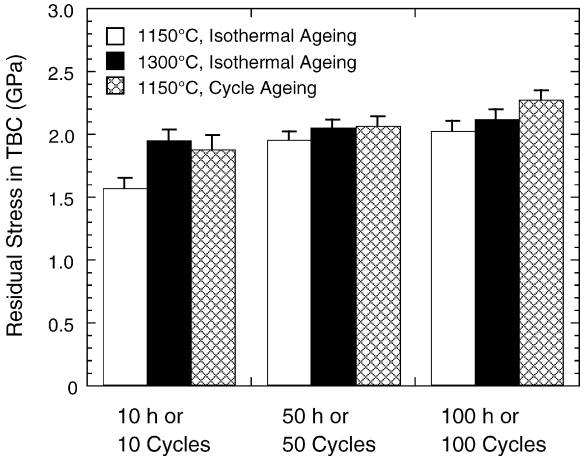

Fig. 7. Comparison of the residual stress in the top coat layer of the EB-PVD TBC system after isothermal and cycle ageing at 1150 and 1300 °C.

increased with aging time and the largest residual stress was observed for the cycle ageing specimen at 1150 °C for 100 cycles. After annealing, the increase of the residual compressive stress is related with an increase in the elastic modulus [16], as result of the sintering effect and reduction of the defect during annealing. The findings indicated that the stresses that built up in TBC layer due to thermal gradient and the mismatch of the thermal expansion coefficient between the top coat and bond coat were larger for cycle ageing than for isothermal ageing, in turn to promote the tetragonal to monocline transformation after cycle ageing at 1150 °C for 100 cycles.

4. Summary

The phase stability of an EB-PVD TBC material was examined after isothermal and cycle ageing at 1150 and 1300 °C up to 100 h and/or 100 cycles using X-ray diffractiometry technique. The following major results are obtained.

The as-deposited EB-PVD TBC material consisted of a nonequilibrum tetragonal phase, t′. After isothermal and cycle ageing at 1150 and 1300 °C, the nonequilibrum tetragonal phase decomposed, dependent on isothermal ageing time and temperature. After isothermal ageing at 1150 °C for 10 h, the t′ phase decomposed to a low Y_2O_3 content tetragonal phase (t1) and a high Y_2O_3 content tetragonal phase (t2). When isothermal ageing time was 50 and 100 h, the t′ phase decomposed to the cubic phase (c), t1 and t2. During isothermal ageing at 1300 °C, the t′ phase decomposed to the t1, t2, and c phases. After cycle ageing at 1150 °C, the t′ phase decomposed to the t1 and t2 for 10 and 50 cycles, while the t′ phase decomposed to the t1, t2 and monocline phase (m) for 100 cycles. After cycle ageing at 1150 °C for 100 cycles, the t′ → m phase transformation was associated with the largest residual stress in the TBC compared to the other ageing TBC materials.

References

[1] G.W. Goward, Progress in coatings for gas turbine airfoils, Surf. Coat. Technol. 108–109 (1998) 73–79.
[2] P.K. Wright, Influence of cyclic strain on life of a PVD TBC, Mater. Sci. Eng. A245 (1998) 191–200.
[3] B.Z. Janos, E. Lugscheider, P. Remer, Effect of thermal aging on the erosion resistance of air plasma sprayed zirconia thermal barrier coating, Surf. Coat. Technol. 113 (1999) 278–285.
[4] E. Tzimas, H. Mullejans, S.D. Peteves, J. Bressers, W. Stamm, Failure of thermal barrier coating systems under cyclic thermomechanical loading, Acta Mater. 48 (2000) 4699–4707.
[5] W. Beele, G. Marijnissen, A. van Lieshout, The evolution of thermal barrier coatings-status and upcoming solutions for today's key issues, Surf. Coat. Technol. 120/121 (1999) 61–67.
[6] M. Peters, C. Leyens, U. Schulz, W.A. Kaysser, EB-PVD thermal barrier coatings for aeroengines and gas turbines, Adv. Eng. Mater. 3 (4) (2001) 193–204.
[7] U. Schulz, K. Fritscher, M. Peters, EB-PVD Y_2O_3- and CeO_2/Y_2O_3-stabilized zirconia thermal barrier coatings-crystal habit and phase composition, Surf. Coat. Technol. 82 (1996) 259–269.
[8] H.G. Scott, Phase relationships in the zirconia-yttria system, J. Mater. Sci. 10 (1975) 1527–1535.
[9] U. Schulz, Phase transformation in EB-PVD yttria partially stabilized zirconia thermal barrier coatings during annealing, J. Am. Ceram. Soc. 83 (2000) 904–910.
[10] Y.H. Sohn, E.Y. Lee, B.A. Nagaraj, R.R. Biederman, R.D. Sisson Jr., Microstructural characterization of thermal barrier coatings on high pressure turbine blades, Surf. Coat. Technol. 146–147 (2001) 132–139.
[11] J. Moon, H. Choi, H. Kim, C. Lee, The effects of heat treatment on the phase transformation behavior of plasma-sprayed stabilized ZrO_2 coatings, Surf. Coat. Technol. 155 (2002) 1–10.
[12] M.H. Li, X.F. Sun, S.K. Gong, Z.Y. Zhang, H.R. Guan, Z.Q. Hu, Phase transformation and bond coat oxidation behavior of EB-PVD thermal barrier coating, Surf. Coat. Technol. 176 (2004) 209–214.
[13] B. Preauchat, S. Drawin, Isothermal and cycling properties of zirconia-based thermal barrier coating deposited by PECVD, Surf. Coat. Technol. 146/147 (2001) 94–101.
[14] K. Wada, N. Yamaguchi, H. Matsubara, Crystallographic texture evolution in ZrO_2-Y_2O_3 layers produced by electron beam physical vapor deposition, Surf. Coat. Technol. 184 (2004) 55–62.
[15] J.R. Brandon, R. Taylor, Phase stability of zirconia-based thermal barrier coatings. Part I. Zirconia-yttria alloys, Surf. Coat. Technol. 46 (1991) 75–90.
[16] A. Portinha, V. Teixeira, J. Carneiro, M.G. Beghi, C.E. Bottani, N. Franco, R. Vassen, D. Stoever, A.D. Sequeira, Residual stresses and elastic modulus of thermal barrier coatings graded in porosity, Surf. Coat. Technol. 188–189 (2004) 120–128.
[17] T. Tomimatsu, Y. Kagawa, S.J. Zhu, Residual stress distribution in electron beam-physical vapor deposited ZrO_2 thermal barrier coating layer by Raman spectroscopy, Metall. Mater. Trans. A. 34A (2003) 1739–1741.